Impedance Theory and Measurements on Porous Acoustic Liners

Andrew B. Bauer*
Douglas Aircraft Company, Long Beach, Calif.

The impedance of a point-reacting liner consisting of a thin, porous surface sheet backed by cavities filled with air or with porous materials has been predicted mathematically for a duct with flow. The mathematical model has been compared with experimental results obtained by using the two-microphone technique for various liners mounted in a 1-ft^2 duct with flow at Mach numbers of 0 to 0.6. The predicted and the measured sound pressures were found to be in good agreement for liners consisting of a single layer of either air-filled or porous cavities covered by a thin porous sheet. As expected, the porous-cavity liners have a wider attenuated bandwidth and a higher attenuation at high frequencies than the air-cavity liners. Since porous cavities might be considered to be the equivalent of a large number of layers of air spaces separated by layers of porous plates, several such multilayer liners were constructed and tested. However, the multilayer liners did not perform like a porous-cavity liner, and a full understanding of the operation of the multilayer liners is yet to be attained.

Introduction

LINER impedance is the critical parameter that determines the amount of sound absorption in an aircraft engine duct. Present-day liners generally consist of a single layer of air-filled cavities separated from the duct airflow by a porous facing sheet designed to absorb acoustic energy as acoustic waves pass through the sheet and into the cavities. Typically, the liner is very effective over a bandwidth of about 1 octave, and the attenuation falls off rapidly for frequencies outside of the bandwidth. The root of the problem is that the impedance of a single-layer liner changes rapidly with frequency; hence, a suggested remedy is a multilayer liner configured to have a near-optimum impedance over a bandwidth significantly wider than that possible for a single-layer liner. A logical extension of the multilayer liner is a liner with a very large number of layers, as would be obtained by using a porous material in place of the air cavities. Porous materials are known to be good acoustic energy absorbers over a wide range of frequency, as contrasted to the air cavity of Helmholtz type. This paper has been written to show some of the main effects of using porous materials and multilayer liners as contrasted with air-cavity liners.

Liners may be subdivided into point-reacting and bulk-reacting types,[1] depending on whether waves within the liner are free to travel only normal to the liner surface or in all directions. Since most air-cavity liners are point-reacting, the porous liners tested were made essentially point-reacting by using a number of impervious walls to subdivide the liner into a number of independent areas. This permitted a direct evaluation of the effects of replacing the air cavities by porous materials. A second line of investigation, which has not been done here, would be to study bulk-reacting liners as compared to point-reacting liners of either the air-cavity or the porous-cavity types.

A mathematical model of the acoustic performance of a porous-cavity, point-reacting liner has been developed. Since the porous material resistivity is a parameter that may be set equal to zero, the model may be applied to zero-resistance or air-cavity liners as well. The model includes the effect of a thin, porous plate over the liner surface.

Presented as Paper 76-539 at the 3rd AIAA Aero-Acoustics Conference, Palo Alto, Calif., July 20-23, 1976; submitted Sept. 28, 1976; revision received Jan. 18, 1977.

Index category: Noise; Aeroacoustics.

*Principal Engineer-Scientist. Member AIAA.

Since materials with very fine pores are good acoustic energy absorbers but tend to be mechanically unsuitable for aircraft engine applications, a number of multilayer liners having pores large compared with those of a typical porous material have been built and tested. The test results have been compared with the mathematical model. Air-cavity and porous-cavity liners also have been built, tested, and compared with the mathematical model. The testing has been done using the two-microphone method[2] to find liner impedance and other parameters. The method has been modified to account for the effects of porous materials rather than air only in the liner cavities.

Experimental Setup

An acoustic test duct, illustrated in Fig. 1, has been installed as a part of the 1-ft^2 (0.305 m) wind tunnel, which is located at the Douglas Aircraft Company Aerophysics Laboratory. The duct freestream Mach number is variable over the range of $0 \leq M_\infty < 1.0$, and the duct pressure level is approximately atmospheric. The duct, which is 72 in. (1.829 m) long, is built with permanent sidewalls of clear plexiglas. The upper and lower walls are removable so that the siren and various acoustic liners may be installed to form the 1-ft (0.305 m) duct.

The siren was designed to generate two-dimensional wavefronts invariant across the 1-ft width between the plexiglas sidewalls, as implied by Fig. 1. The waves were generated at the apex of the siren horn, where the rotor served as a valve to alternately open and close a 1-ft-long row of 24 holes of 0.312-in. (7.9-mm) diam. The valve action permits compressed air to enter the horn from the siren housing. The wave amplitude is controlled by the pressure level p_{sir} in the siren housing, which was varied from zero to 10 psi (69,000 Pa) above the test section static pressure. The mass flowrate through the siren was 0.08 kg/s for many of the tests, which were done at $p_{sir} = 1.5$ psi (10,300 Pa), and was 0.20 kg/s for $p_{sir} = 10$ psi. Hence, the mass flow from the siren was much less than the duct flowrate, which was typically 15 kg/s at $M_\infty = 0.4$. For $p_{sir} > 3.0$ psi (20,600 Pa), the wave amplitudes were sufficient that weak shock fronts were formed. Examples of these wave fronts were recorded by the shadowgraph technique and were compared with wavefronts calculated from linear theory. Agreement between the calculations and the shadowgraphs was excellent, as illustrated by the example in Fig. 2. The waves in the figure are numbered in proportion to the time since each wave

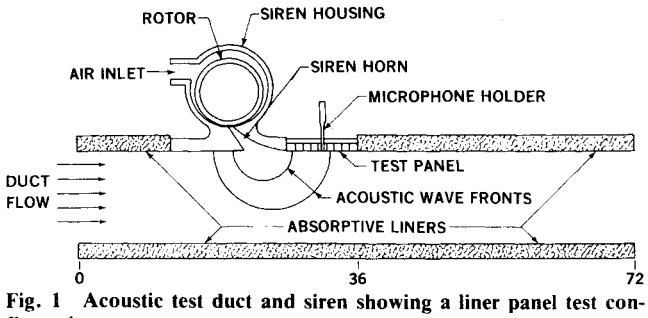

Fig. 1 Acoustic test duct and siren showing a liner panel test configuration.

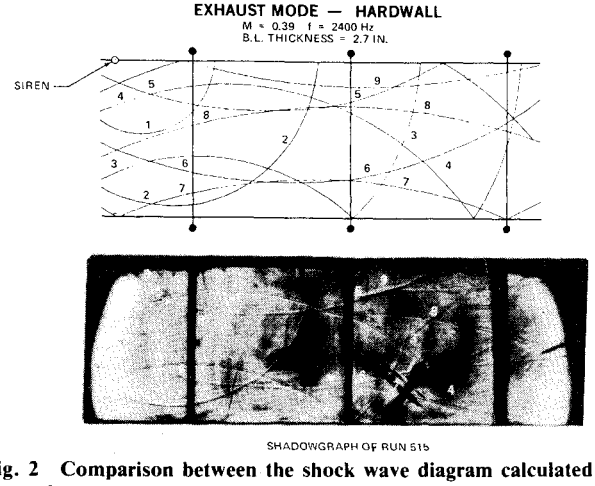

Fig. 2 Comparison between the shock wave diagram calculated by linear theory and a shadowgraph.

emanated from the siren, taken to be a point source. The visible part of wave 9 has been reflected four times, twice from the bottom hardwall and twice from the top hardwall, without being noticeably distorted from its circular shape in spite of traveling four times through $M_\infty = 0.39$ turbulent boundary layers on the two walls. In other examples the lower duct wall was made soft, which resulted in a more complicated wave pattern, but again showing excellent agreement between the calculations and the experiments.

A boundary-layer survey made near the upper wall at station 32 in the duct for $M_\infty = 0.40$ showed a velocity profile very close to the usual 1/7 power shape; the layer thickness was 1.5 in. (38 mm), which corresponds to a distance of about 9 ft (2.75 m) from a virtual origin on a flat plate. However, the distance from the plenum inlet region to station 32 is only about 8 ft (2.44 m), and so the boundary layer evidently was thickened by the siren horn and the perforated liner. The siren was located between stations 12 and 27, the same as in Fig. 1, and the remainder of the upper wall was paneled with a perforated plate liner. No airflow was run through the siren. It is interesting that the boundary layer had the 1/7 power shape in spite of any flow disturbances generated by the siren and the liner.

Of the 20 liners tested, five of them are the air-cavity type, with perforated surface plates, as shown in Fig. 1 and Table 1 of Ref. 3, and designated by the numbers P-513, P-515, P-517, P-519, and P-521. These were mounted one at a time on the test duct, as shown in Fig. 1, and type P-501 perforated liner panels[3] were used to line the remainder of the duct upper surface and all of the lower surface. Unfortunately, as described more fully in Ref. 3, this test arrangement resulted in an undesirably high level of self-noise generation in the duct, caused by the interaction of the boundary layers with the perforated holes. Nevertheless, some testing was done, prinicpally at $M_\infty = 0$ and 0.2. Typical wave shapes are shown in Fig. 3; in each photograph the upper trace is the pressure

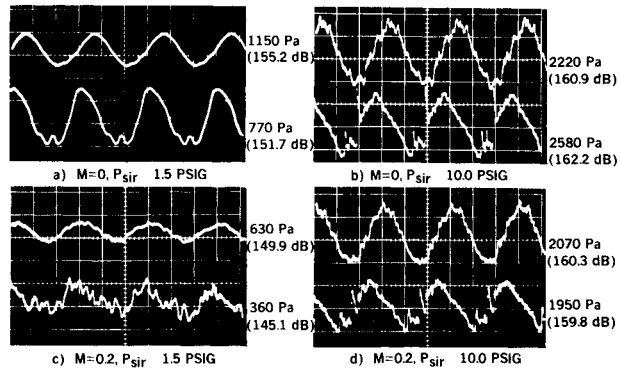

Fig. 3 Waveforms on test liner P-515, $f = 1660$ Hz.

time-history obtained from microphone no. 1, a ⅛-in. (3.2-mm) B&K microphone located at the bottom of one cavity of the test liner; the lower traces were obtained from microphone no. 2, a ⅛-inch (3.2-mm) B&K microphone on the surface of the liner, as implied by the microphone holder in Fig. 1.

In Fig. 3a, taken with no flow in the duct, the waveforms are almost sinusoidal, but Fig. 3b, taken with a higher amplitude from the siren, shows the presence of a number of shock waves, particularly for the lower trace, which is that from the lining surface microphone. The microphone in the lining cavity is partly shielded from the irregular pressure fluctuations on the lining surface; the cavity waveform generally is more sinusoidal than that on the lining surface. In Fig. 3c, it can be seen that for a duct flow Mach number of 0.2, the pressure fluctuations from the duct flow are added to the waveform. Figure 3d shows the effects of both the higher amplitude siren output and the duct flow. Sound pressure levels both in Pascals and in decibels relative to 20×10^{-6} Pa are given to the right of the waveforms. Such waveforms have been digitized and processed by computer to obtain the Fourier series fundamental components, which in turn have been used to calculate the lining impedance.

The pseudosound level generated by a turbulent boundary layer on a flat plate with zero pressure gradient for low-speed flows is given by Willmarth[4] as

$$p_w = 0.005q$$

where q is the dynamic pressure of the freestream, $\gamma p_\infty M_\infty^2/2$. Since p_∞ of the test section is about 10^5 Pa, and since $\gamma = 1.4$, the following is obtained:

$$p_w = 350 M_\infty^2 \text{ (Pa)}$$

Hence, the pseudosound levels are as given in Table 1. These levels are much below those typically generated by the siren, as those in Fig. 3, and represent a possible lower limit to the self-noise generated by a liner. The levels are far below those for the self-noise of the perforated plate liners, where the levels were on the order of 300, 1500, and 750 Pa for $M_\infty = 0.2$, 0.4, and 0.6, respectively.

All of the remaining 15 liners which were tested were designed with surface openings that are, at most, only a few thousandths of an inch in diameter, in contrast with the 0.156-in.-(4-mm) diam holes of the perforated plate liners, with the intent of greatly reducing the self-noise to levels near those in Table 1. This effort generally was a sucess, since the self-noise

Table 1 Turbulent boundary-layer pseudosound levels

M_∞	p_w, Pa	p_w, dB
0.2	14	116.9
0.4	56	128.9
0.6	126	136.0

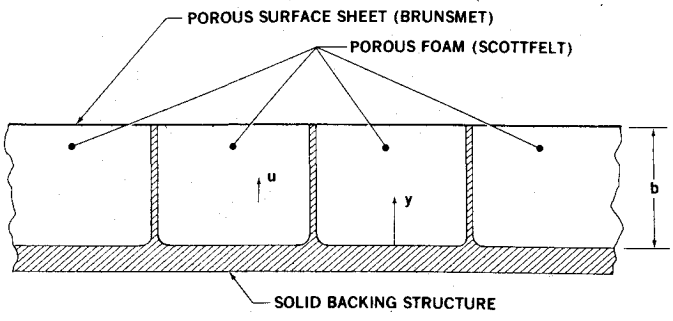

Fig. 4 Cross-sectional sketch of a porous liner construction.

level turned out to be near 100 Pa for $M_\infty = 0.2$ and near 200 Pa for $M_\infty = 0.4$ and 0.6, which is encouraging in view of the perforated liner values and the lower limits given by Table 1.

Seven of the 15 liners were constructed as illustrated in Fig. 4. The liner cavities were filled with Scottfelt foam of various grades. The thin surface sheets were Brunsmet, which consists of a thin mat made up of many 8-μ-diam stainless steel wires sintered together and bonded to a perforated plate having an open area ratio of 0.35. The plate is then used only for the purpose of supporting the mat, which is the part exposed to the airstream. The mat surface is very flat and smooth to the touch, which helps to account for the low self-noise levels. The Brunsmet material has a thickness of 0.025 in. (0.63 mm) and was used in several grades, which had flow resistance ratings of either 100, 200, or 400 mks rayls.

Six of the remaining eight liners had surfaces made up of Brunsmet; the other two were made entirely of resin-impregnated woven fiberglass. The six liners had one or more layers of air-filled cavities separated by layer(s) of either Scottfelt, Brunsmet, or perforated plate(s).

For the tests of each of the 15 Brunsmet and the woven fiber-glass test panels, shown in Fig. 1, the linings, which extend along the upper surface from stations 0 to 12 and stations 36 to 72, were made up of a 2-in. layer of Scottfelt 2-900 covered with a Brunsmet surface having a flow resistance of 100 mks rayls. The same construction was used for the entire lower surface of the duct.

All of the liners were tested, as illustrated in Fig. 1, using microphone no. 1 at the bottom of the liner cavity and microphone no. 2 on the liner surface. Because of the two-dimensional nature of the wavefronts, the two microphones could be moved perpendicular to the plane of the paper in Fig. 1 without affecting the microphone outputs. This permitted the surface microphone to be placed some distance away from the cavity microphone in order to minimize the effect of the surface microphone holder, which extends through the cavity, on the cavity microphone output.

For the tests of the 15 Brunsmet and the woven fiberglass panels, the microphone signals were passed through narrowband filters, which were then used to calculate liner impedance parameters, which are a function of the siren pressure p_{sir} and liner sound pressure levels, as well as other factors. The effects of noise at other than the siren frequency, which may interact in a nonlinear manner with the siren frequency energy, were not evaluated for these experiments.

Mathematical Model of Liner Performance

A mathematical model is needed to relate the two-microphone measurements to liner impedance. A model has been developed for air-cavity liners[2,5]; the model is extended here to apply to porous, point-reacting liners.

Governing Equations within the Porous Material

The equations of motion and mass conservation in a porous medium have been discussed by Nayfeh et al.[1] and earlier by Zwikker and Kosten.[6] For a point-reacting liner material they are

$$\rho_e \frac{\partial u}{\partial t} + Ru + \frac{\partial p}{\partial y} = 0 \tag{1}$$

$$\Omega \frac{d\rho}{dp} \frac{\partial p}{\partial t} + \rho_0 \frac{\partial u}{\partial y} = 0 \tag{2}$$

where R is the porous media resistivity, ρ_0 is the density of the ambient gas, ρ_e is the effective density of gas in the porous media, and Ω is the porosity, defined as the ratio of void volume to total bulk volume of the material. The effective density usually is given as

$$\rho_e = s\rho_0/\Omega \tag{3}$$

where s is a structure factor, which accounts for the apparent increase in the air density as a result of the passage of the air around constrictions in the material. The acoustic pressure and density are related by

$$dp/d\rho = c_e^2 \tag{4}$$

where c_e is the effective speed of sound. In general, c_e is a complex number[6]; it is real and equal to the adiabatic speed of sound only when the porous Reynolds number

$$R_p = \omega\rho_0 r^2/\mu \tag{5}$$

is much greater than 1; c_e is real and equal to the isothermal speed of sound when R_p is much less than 1. For the remainder of this paper, the simplifying assumption that $c_e = c$, where c is a real number, will be used. Also, as illustrated in Fig. 4, y is the coordinate normal to the solid backing structure, and b is the liner backing or porous material depth.

Now the momentum equation is satisfied if

$$u = \partial\Phi/\partial y \tag{6}$$

$$p = -\rho_e(\partial\Phi/\partial t) - R\Phi \tag{7}$$

where Φ is an unknown function. By putting Eqs. (4, 6, and 7) in Eq. (2), the result is the modified wave equation

$$\frac{\Omega}{c^2}\frac{\rho_e}{\rho_0}\frac{\partial^2\Phi}{\partial t^2} + \frac{\Omega R}{\rho_0 c^2}\frac{\partial\Phi}{\partial t} - \frac{\partial^2\Phi}{\partial y^2} = 0 \tag{8}$$

which has a solution in the form

$$\Phi = e^{i\omega t} f(y) \tag{9}$$

Boundary Condition

In order to satisfy the differential equation and the boundary condition $u = 0$ at $y = 0$, the following equation is used:

$$\Phi = A_0 e^{i\omega t}\{(\cos k_1 y)\cosh k_2 y + i(\sin k_1 y)\sinh k_2 y\} \tag{10}$$

where

$$k_1 = kK_1 \qquad k_2 = kK_2$$

$$k = \omega/c = 2\pi f/c$$

$$K_1 = \{s/2 + \tfrac{1}{2}[s^2 + \Omega^2 r^2]^{\frac{1}{2}}\}^{\frac{1}{2}}$$

$$K_2 = \Omega r/2K_1 \qquad r = R/\omega\rho_0$$

Using Eq. (10) in Eqs. (6) and (7), the particle velocity and acoustic pressure are obtained

$$u = A_0 e^{i\omega t}(k_2 + ik_1)\{(\cos k_1 y)\sinh k_2 y + i(\sin k_1 y)\cosh k_2 y\} \quad (11)$$

$$p = -iA_0 e^{i\omega t}(s - i\Omega r)(\rho\omega/\Omega)\{(\cos k_1 y)\cosh k_2 y + i(\sin k_1 y)\sinh k_2 y\} \quad (12)$$

Liner Impedance

The specific acoustic impedance of the cavity porous material measured at $y = b$ is

$$\zeta_c = -(p/\rho c u)_{y=b} = GH/\sin kb \quad (13)$$

where

$$G = (\cos k_1 b)\cosh k_2 b + i(\sin k_1 b)\sinh k_2 b \quad (14)$$

$$H = -\frac{i(K_1 - iK_2)\sin kb}{\Omega\{(\sin k_1 b)\cosh k_2 b - i(\cos k_1 b)\sinh k_2 b\}} \quad (15)$$

and the specific acoustic impedance of the liner is

$$\zeta = GH/\sin kb + \theta_s + i\chi_s \quad (16)$$

where θ_s and χ_s are the specific acoustic resistance and reactance of the thin surface sheet shown in Fig. 4. Notice that, as the cavity porous material approaches zero density, so that Ω and $s \to 1$ and $r \to 0$, the result is $G \to \cos kb$, $H \to -i$, and $\zeta_c \to -i\cot kb$, which is the solution for an air-filled cavity.

Expressions for θ_s and χ_s

A number of papers, Refs. 7-11, for example, have given various expressions for the specific acoustic resistance and reactance of liner surfaces. From these and other results, a useful representation for θ_s has been obtained as follows:

$$\theta_s = \theta_0 + \theta_1 + \theta_2 M_n + \theta_3 M_\infty \quad (17)$$

Here θ_0 is the resistance for surfaces with holes so small that the flow is completely viscous and the porous Reynolds number R_p [see Eq. (5)] is much less than 1. The resistance $\Delta p/\rho c u_s$ often is obtained by measuring the pressure drop Δp and the steady flow velocity u_s through the surface sheet in the limit as u_s goes to zero. For example, a Brunsmet sheet with a steady flow rating $\Delta p/u_s$ of 200 mks rayls would have $\theta_0 = 0.5$.

For surfaces with holes that are large enough so that R_p is much greater than 1, and thus the flow is not completely viscous, the specific acoustic resistance is

$$\theta_1 = [(8\mu\rho\omega)^{1/2}/\sigma\rho c](1 + t/d) \quad (18)$$

which was obtained by Ingard,[12] where t is the surface sheet thickness, d is the diameter of the holes, and σ is the ratio of open or hole areas to total area. Since θ_0 and θ_1 both are used to represent the resistance, depending on whether R_p is much smaller or much larger than 1, θ_0 must be 0 when $R_p \gg 1$ and θ_1 must be 0 when $R_p \ll 1$. Further work needs to be done to determine θ_0 and/or θ_1 for R_p near or equal to 1. For a Brunsmet sheet R_p usually is much less than 1, whereas for perforated plates R_p generally is much greater than 1; however, for other materials R_p may be on the order of 1.

The resistance $\theta_2 M_n$ is the nonlinear effect, which results from large values of u_n, the rms amplitude of the acoustic velocity normal to the liner surface, and the corresponding Mach number, $M_n = u_n/c$. For a sheet with circular orifices, Zinn[13] obtained the expression

$$\theta_2 M_n = 1.15 M_n/\sigma^2 \quad (19)$$

which again works well for perforated sheets, as shown by Zinn's comparison with experiments, but is open to question for sheets like Brunsmet with very fine pores.

The term $\theta_3 M_\infty$ is the "grazing flow" effect, a result of the freestream and boundary-layer flow over the liner. In order to measure this effect, a number of steady-flow experiments[14-16] have been run in which the pressure difference across a perforated sheet has been obtained as a function of $M_\infty, M_1, \sigma, t/d$, δ/d, and R_d, where M_1 is the average Mach number of the mass flow through the holes, δ is the boundary-layer thickness, and R_d is the Reynolds number based on $M_\infty c$ and d. The pressure difference can be defined as $p_\infty - p_b$, where p_∞ is the freestream pressure and p_b is the pressure on the cavity side of the sheet at some distance from the hole. As suggested by Bauer,[7] the data may be organized in a simple manner by nondimensionalizing the pressure differences and plotting them as a function of M_1/M_∞. This is done by defining

$$C_p = \frac{2(p_\infty - p_b - p_0)}{\gamma p_\infty M_\infty^2} = \frac{2\Delta p}{\gamma p_\infty M_\infty^2} \quad (20)$$

where γ is the specific heat ratio ($\gamma = 1.4$ for air), and p_0 is the value of $(p_\infty - p_b)$ for $M_1 = 0$. Here M_1 is defined positive for flow away from the grazing stream. Note that, for zero orifice flow, the asymmetry of the grazing flow causes p_∞ to be different from p_b, so that p_0 is not zero. Evidently because p_0 is quite small compared to p_∞, p_0 already has been subtracted out of the data presented in Refs. 14 and 16, and the actual value of p_0 seems to have little practical consequence. Figures 5 and 6 show typical plots of C_p as a function of M_1/M_∞. The data in Figs. 5 and 6 and other related plots can be represented in the form

$$C_p = G_3\left(\frac{M_1}{M_\infty}\right) + G_2\left(\frac{M_1}{M_\infty}\right)\left|\frac{M_1}{M_\infty}\right| \quad (21)$$

where G_2 and G_3 are weak functions of the nondimensional parameters M_∞, σ, t/d, δ/d, R_d, and the sign of M_1. If Eq. (21) is multiplied by $V_\infty^2/(2c^2 M_1 \sigma)$, where $cM_1 = V_1$, the result is

$$\frac{C_p V_\infty^2}{2c^2 M_1 \sigma} = \frac{\Delta p}{\rho_\infty c V_1 \sigma} = \frac{G_3 M_\infty}{2\sigma} + \frac{G_2 |M_1|}{2\sigma} \quad (22)$$

which is the result of steady-flow experiments. The assumption can be made that this equation applies for oscillatory flows, as discussed in Ref. 16. Since $\Delta p/(\rho_\infty c V_1 \sigma)$ is of the form of specific acoustic resistance, and since $M_n = M_1/\sigma$, the result is

$$\theta_2 = G_2/2\sigma^2 \quad (23)$$

$$\theta_3 = G_3/2\sigma \quad (24)$$

Note that the absolute value sign of M_1 must be dropped in changing Eq. (22) from a steady-flow to an oscillatory flow result.

For parameter values typical of perforated sheet liners, that is, for

$$M_\infty < 0.7 \qquad M_1 < 0.1 \qquad 0.02 < \sigma < 0.20$$

$$0 < t/d < 1 \qquad 2 < \delta/d < \infty$$

the available experimental data give the value $G_3 = 0.6$, and seem to support the value $G_2 = 2.3$, so that Eq. (19) and (23)

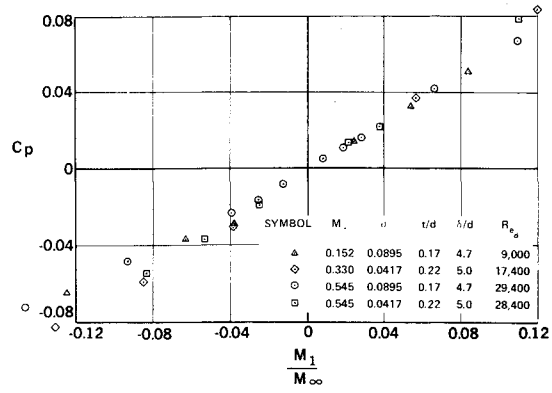

Fig. 5 Pressure coefficient vs orifice Mach number ratio (data from Ref. 14).

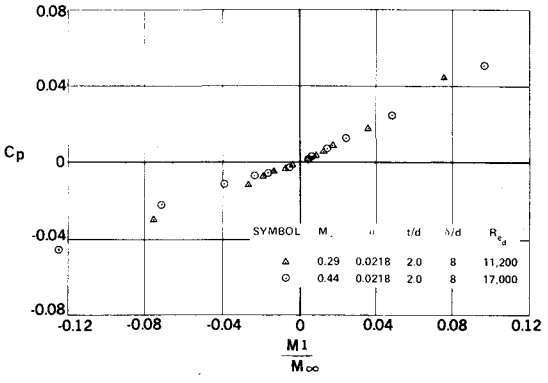

Fig. 6 Pressure coefficient vs orifice Mach number ratio (data from Ref. 15).

are in agreement. Note that Fig. 6, for which $t/d=2$, indicates that $G_3=0.52$ for M_l positive and 0.38 for M_l negative. This corresponds to the fact that levels of Δp on the right- and the left-hand sides of the $M_n=0$ line in Fig. 7c of Ref. 15 are different, which has caused some controversy. A similar but less significant effect is noticeable in Fig. 5. In contrast, the data of Ref. 16, which were taken for single square orifices with $t/d=1.0$ and $\delta/d=0.7$, give $G_3=1.3$.

Rice,[11] in an approximate theoretical study of grazing flow, has found θ_3 to be 0.5, which compares favorably with $G_3/2=0.3$ from Fig. 5. For M_l positive and steady flow, Rice found that the orifice discharge coefficient was, approximately,

$$c_D=(M_l/M_\infty)^{1/2} \tag{25}$$

which, since $C_p=(V_l/V_\infty c_D)^2$, corresponds to $G_3=1.0$. Dean[17] reports that $\theta_3\sigma$, which is a_l in his terminology, is about 0.3 based on experimental data.

Considering all of the preceding material, the value of $\theta_3\sigma$ is believed to be about 0.3 for the typical perforated sheet liner, but for other surface sheet configurations, such as Brunsmet or woven fiberglass, the value of θ_3 should be determined through experiments.

A number of different expressions for the specific acoustic reactance of a perforated liner surface have appeared in the literature, where a major problem is that of evaluating the "end effect" of an orifice flow. As a starting point, it can be assumed that the flow is inviscid and that the end effects are zero; then the surface sheet impedance is a pure reactance given by

$$\chi_s=\frac{(\tan kt)\,(1+\sigma^2\cot^2 kb)}{\sigma[1+\sigma(\cot kb)\tan kt]} \tag{26}$$

which is valid for a surface sheet of any thickness t, whether large or small, and for an air-filled cavity of depth b. Since the terms $\sigma^2\cot^2 kb$ and $\sigma(\cot kb)\tan kt$ usually are small as compared to 1, Eq. (26) can be written as

$$\chi_s=(l/\sigma)\tan kl \tag{27}$$

as used by Bell et al.,[8] where t has been replaced by the effective length l, which is larger than t by the amount of the end effect on the orifice flow. Since kl usually is small as compared to 1, χ_s usually is written as

$$\chi_s=kl/\sigma \tag{28}$$

Various expressions have been given for l. An often cited expression is

$$l=t+0.85\delta_0 d(1-0.71\sigma^{1/2}) \tag{29}$$

which was given by Garrison.[18] The factor δ_0 is 1.0 for "small" values of M_∞ and M_n, but it decreases to 0.38 for larger values of these parameters, as discussed by Bell et al.[8] However, recently published information suggests that l may be represented more simply by

$$l=t+a_0 d \tag{30}$$

where a_0 is an end effect factor. Rice[11] has calculated the value $a_0=0.25$ for grazing flows. Dean[17] suggests, based on experiments, that a_0 should be about 0.25 for grazing flows above 30 m/s and 0.50 for zero grazing flow. Experiments by the author also have indicated that a_0 is about 0.25 for grazing flows and somewhat higher without grazing flow. If $\sigma=0.1$ and $\delta_0=0.38$ in Eq. (29), the second term on the right-hand side reduces to $0.25d$, which is in complete agreement with the grazing flow results quoted for Eq. (30). Hence, Eq. (30) appears to be a simple and useful representation of l where $a_0=0.25$ for most grazing flow conditions and $a_0>0.25$ when grazing effects are "small" by some measure. For materials such as Brunsmet, where σ and d are not easily defined, because of the small size of the pores or holes, some type of experiment is required to determine χ_s.

Obtaining Liner Impedance Using the Two-Microphone Method

As described earlier, the two-microphone test arrangement has been used with either digital processing or narrowband filtering to obtain the first Fourier components of each pressure signal, which may be written in the form

$$P_l=\sqrt{2}Ae^{i\omega t} \qquad P_2=\sqrt{2}Be^{i(\omega t+\phi)} \tag{31}$$

for the cavity and the liner surface microphones, respectively. The measured parameters A, B, and ϕ are used to obtain liner impedance as a function of duct-flow Mach number, frequency, sound pressure level, and liner geometry. The rms sound pressure level on the liner surface is, of course, equal to B; and the duct Mach number and test frequency are known from the test setup. The liner impedance may be calculated from the equation

$$J=\frac{\sin kb}{H}\zeta=G+\frac{\sin kb}{H}(\theta_s+i\chi_s)=\frac{Be^{i\phi}}{A} \tag{32}$$

In practice, the experimental values of B/A and ϕ are plotted as functions of the dimensionless frequency kb, and these functions are compared with calculations made for the amplitude and the argument of J. Since the parameters Ω, s, r, θ_s, and χ_s, which are used to compute J, are known only to some degree of approximation, some iteration of the calculations generally is necessary to find values of the input

Table 2 Liner design data

Identification number	Cavity material	Cavity depth b, in.	Surface sheet material
P-515	Air	0.650	Perforated $t=0.040$ in., $d=0.156$ in., $\sigma=0.0652$
P-519	Air	0.351	Perforated $t=0.040$ in., $d=0.156$ in., $\sigma=0.0392$
517	Air	0.750	Brunsmet, 400 mks rayls
519	Scottfelt 2-900	2.000	Brunsmet, 100 mks rayls
527	5 layers – air layers alternating with perforated plate	0.830	Brunsmet, 200 mks rayls
529	11 layers – air layers alternating with perforated plate	0.875	Brunsmet, 200 mks rayls

parameters so that computed values of J are in agreement within experimental accuracy with the measurements.

Experimental Results

Experimental results are given here for several different liner types, whose construction is summarized in Table 2. The experimental data are compared with predictions by using Eq. (32) and the appropriate input data.

Air-Cavity with a Brunsmet Surface (Liner 517)

Because of its air-filled cavities, liner 517 has $\Omega=s=1$ and $r=0$, so that only θ_s and χ_s need be estimated for computing J. Figures 7 and 8 show the experimental values of B, B/A, and ϕ as functions of M_∞ and kb. Also shown are corresponding values of $|J|$ and Arg J. These were calculated using Eq. (17) and (28) with $\theta_1=\theta_2=0$ and $l/\sigma=0.50$ in. The Brunsmet rating of 400 mks rayls implied that $\theta_0=1.0$, but θ_0 had to be increased to 1.25 to obtain reasonable agreement between J and $Be^{i\phi}/A$. Since σ was unknown for the Brunsmet material, values of l/σ were varied until satisfactory agreement with experimental results, but the scatter of the results is such that the true value of θ_3 cannot be scatter picked with precision. The parameters θ_0 and l/σ were varied simultaneously to obtain the results shown, as any change in either parameter affected both $|J|$ and Arg J. Hence, the main results of the testing were the experimentally determined values of θ_s and χ_s through the parameters θ_0, θ_3, and l/σ.

Experimental values of B are shown in hundreds of Pascals beside the data points in Figs. 7 and 8. Note that 200 Pa corresponds to 140 dB and that 2000 Pa corresponds to 160 dB. When the siren pressure was reduced to zero, the overall rms sound pressure level (SPL) on the liner surface was found to be 97, 225, and 245 Pa for $M_\infty=0.2$, 0.4, and 0.6, respectively. Hence, the flow noise, which was a broadband noise, was much lower in any given narrow-frequency band than the SPL in that same band generated by the siren.

Scottfelt-Cavity Liner with a Brunsmet Surface (Liner 519)

Liner 519 has a 2.00-in.-deep cavities filled with a Scottfelt porous foam of grade 2-900, which can be compressed to more than 10 times its initial thickness, indicating an open volume ratio of $\Omega>0.90$. For this reason $\Omega=0.9333$ was chosen in comparing experimental and calculated results. These are shown on Figs. 9 and 10. Notice that J is a function of both M_∞ and p_s, where p_s is the rms sound pressure level on the liner surface; however, for an air-filled liner, as in Figs. 7 and 8, J does not depend on p_s. This is a result of the fact that the Scottfelt resistance parameter r is a function of u, and that u is a function of p_s. Data supplied by the Scott Company were used in the equation

$$R=\Delta p/v\Delta y \tag{33}$$

to compute R, where Δp is the pressure drop across a piece of foam of thickness Δy with a steady-flow velocity v through the foam surface. Then R was used in Eq. (10) with the result

$$r=(2400+720v)/f=(r_1+r_2v)/f \tag{34}$$

where f is the frequency in Hertz and v is the velocity in meters per second. For the calculated results, r was taken to be in the form of Eq. (34) and v as the rms value of the acoustic

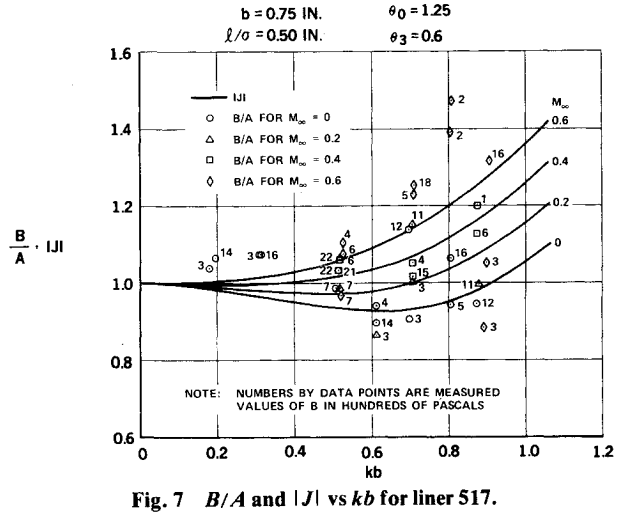

Fig. 7 B/A and $|J|$ vs kb for liner 517.

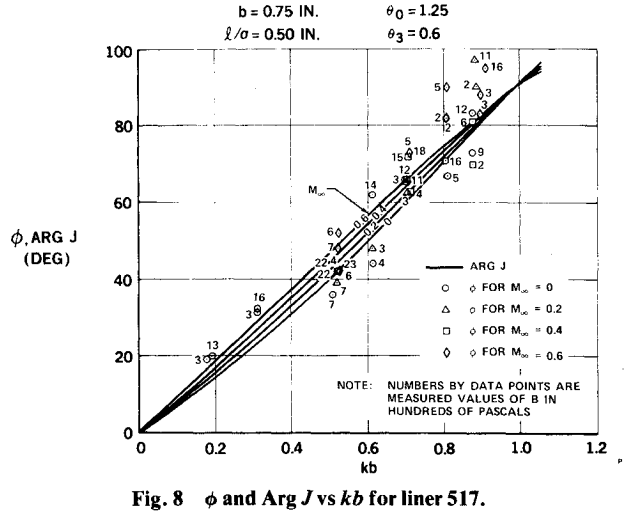

Fig. 8 ϕ and Arg J vs kb for liner 517.

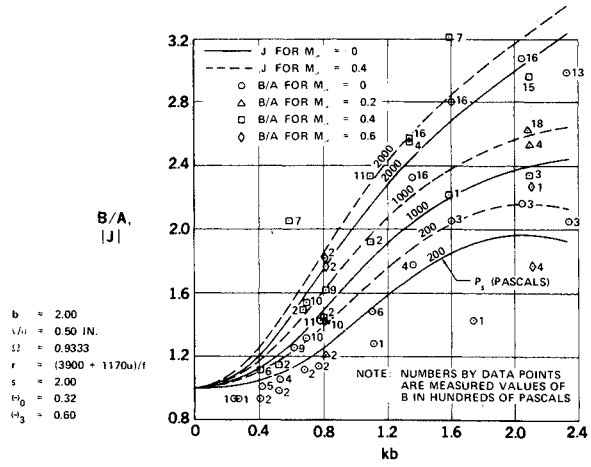

Fig. 9 B/A and $|J|$ vs kb for liner 519.

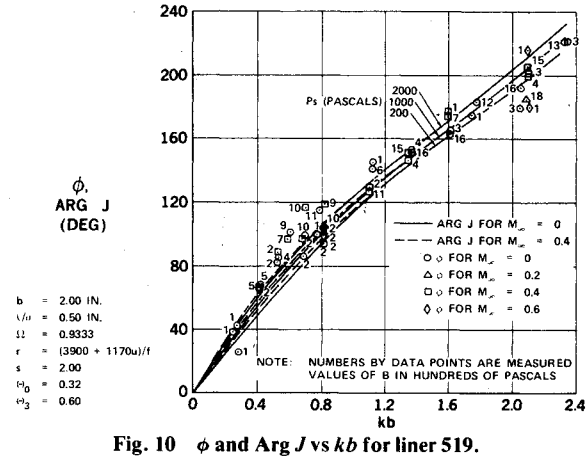

Fig. 10 ϕ and Arg J vs kb for liner 519.

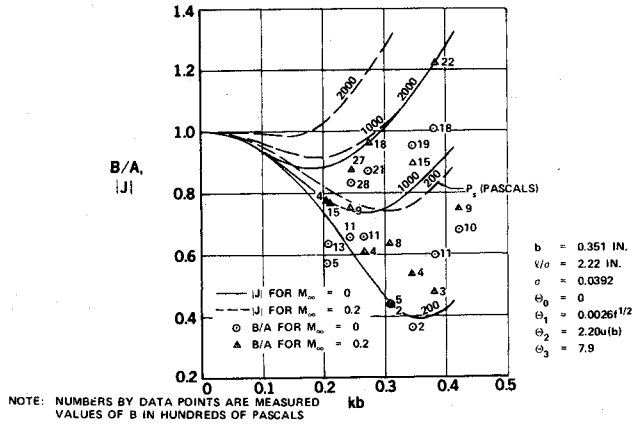

Fig. 11 B/A and $|J|$ vs kb for liner P-519.

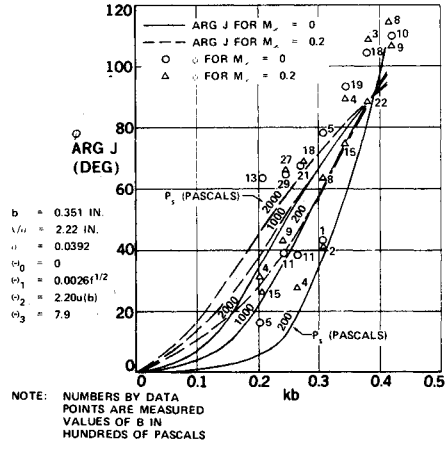

Fig. 12 ϕ and Arg J vs kb for liner P-519.

velocity. Then r_1, r_2, and s were varied until the experiments and the calculations agreed, as shown in Figs. 9 and 10. For this operation, r_2 was maintained equal to 0.30 r_1, and then r_1 and s were varied to fit the data. As was known by its definition, s had to be larger than 1. The final values were $r_1 = 3900$/s, $r_2 = 1170$/m, and $s = 2.0$. As may be seen in the figures, the agreement between calculations and experiments was generally good, indicating that the solution to the differential equations was representative of the physical processes of the fluid flow in a porous liner.

Throughout the calculations, Eqs. (17) and (28) were used for the impedance of the Brunsmet surface plate. As had been found using liner 517, l/σ was taken to be 0.50 in., and θ_0 was equal to 0.32, or 25% larger than the value obtained based on manufacturer's rating of 100 mks rayls. θ_3 was taken to be 0.6, which again is the right order of magnitude to give a reasonable fit to the scattered data points in Fig. 10. With the siren turned off, the flow noise levels on the liner surface were 90, 210, adn 235 Pa for $M_\infty = 0.2$, 0.4, and 0.6, respectively.

Air-Cavity Liner with a Perforated Sheet Surface (Liner P-519)

Experimental and calculated results for liner P-519 are shown in Figs. 11 and 12. The calculations were performed using $\theta_0 = 0$, $\theta_1 = 0.199\ (kb)^{1/2}$, $\theta_2 = 748$, and $\theta_3 = 7.91$ in Eq. (17) for θ_s. These values for the θ's were obtained using Eqs. (18, 19, and 24). Also, $a_0 = 0.3$ was used in Eqs. (28) and (30) to obtain χ_s. The comparison in Fig. 11 indicates general agreement between B/A and $|J|$ in Fig. 11 for the $p_s = 200$ Pa and for $M_\infty = 0$; however, for p_s in the range of 1000 to 2000 Pa, the B/A values generally are smaller than $|J|$, which indicates that θ_2 should be decreased by about 25% from that given by Eq. (19). The M_∞ parameter θ_3 is much too large for good agreement. Tests of another perforated liner, P-515, also indicate that θ_3 should be much smaller than that given by Eq. (24) with $G_3 = 0.6$. Hence, for these two liners, the data indicate that the grazing flow effect is much less than expected.

Figure 12 shows general agreement between ϕ and Arg J, although the scatter and inconsistency of the data prevent any precise comparison. It is interesting that both the data and the calculations show that, for the perforated sheet liner, the relation between ϕ or Arg J and kb is more nonlinear than for the Brunsmet sheet liner, shown in Fig. 8. The characteristics of the curves are such as to reduce the absorptive bandwidth of the perforated sheet liner in comparison to the Brunsmet sheet liner. With the siren off, the flow noise levels on the surface of liner P-519 were 250 and 1060 Pa for $M_\infty = 0.2$ and 0.4, respectively.

Perforated-Plate Cavity Liner with a Brunsmet Surface (Liner 529)

As indicated by Table 2, liner 529 was built with a "cavity" section consisting of 11 layers. Six of the layers are air spaces, each with a thickness of 0.125 in. (3.2 mm). The six air layers are alternated with five perforated sheet layers, each having a thickness of 0.025 in. (0.64 mm) and an open area ratio of 0.21; the hole diameters are 0.046 in. (1.2 mm). The sheets were aligned so that the holes of all sheets were in line with each other. The intent of this structural design has been to simulate the acoustic behavior of a porous material without using very fine pore sizes, as would be obtained using an acoustic foam. The perforated plate structure was judged to be more practical than foam for aircraft applications, where fluid contamination of the liner may be a problem.

Figures 13 and 14 show the experimental data and curves of $|J|$ and Arg J calculated for constant values of p_s. Since the

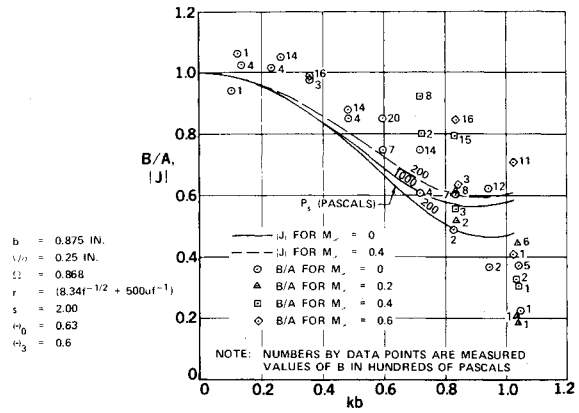

Fig. 13 B/A and $|J|$ vs kb for liner 529.

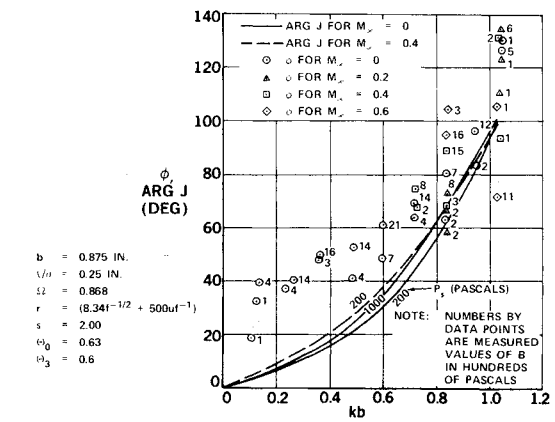

Fig. 14 ϕ and Arg J vs kb for liner 529.

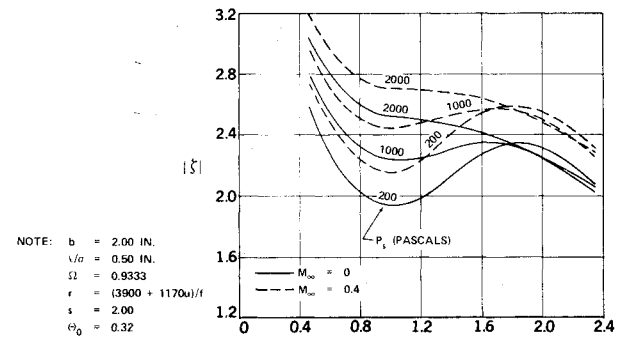

Fig. 15 Calculated $|\zeta|$ vs kb for liner 519.

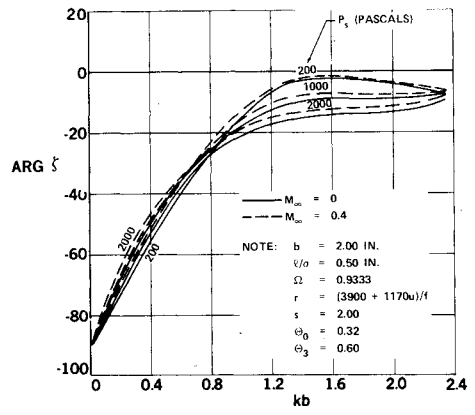

Fig. 16 Calculated Arg ζ vs kb for liner 519.

liner surface material is Brunsmet with a 200 mks rayl rating, half the value of liner 517, θ_0 was taken to be 0.63. Also, it was assumed that $\theta_1 = \theta_2 = 0$, $\theta_3 = 0.6$, and $l/\sigma = 0.50$ in. (13.6 mm). The volume ratio $\Omega = 0.868$, and s was at first estimated to be 1.63. The parameter r was estimated to be $(8.34 f^{-1/2} + 1000 v f^{-1})$, based on the perforated plate resistance functions described earlier. Since these parameters resulted in a bad match between the calculations and the experiments, the values of r, s, and l/σ were varied to find a better match. This was only partly successful, as shown on the figures. The figures were calculated using $r = (8.34 f^{-1/2} + 500 v f^{-1})$, $s = 2.0$, and $l/\sigma = 0.25$ in. The crux of the problem appears to be the resistance paramter θ_0. To obtain better agreement, θ_0 needs to be small at high frequencies, kb near 1.0, so that $|J|$ can be as small as B/A; however, at low frequencies, $kb < 0.5$, θ_0 needs to be large, so that Arg J can be larger to match ϕ. This brings into question whether the equation $\theta_s = \theta_0 + \theta_3 M_\infty$ is the correct form for Brunsmet material; perhaps the θ_0 term should vary with frequency through some mechanism. Notice that, when θ_1 is made nonzero, it varies like $f^{1/2}$, as given by Eq. (18), which is opposed to the direction that θ_s must follow if the experimental data are to be matched.

Since this matching problem could not be resolved in any simple manner, the data were examined for any obvious errors, but none could be found. In fact, the data are remarkably self-consistent in view of the greater amount of inconsistency in the data of Figs. 7-12. Furthermore, when the data of liner 527, which was designed to be quite similar to liner 529 except for the reduction in the number of layers, were examined, it was found that the liner 527 data have the same general characteristics as shown for liner 529. The two perforated plates in the cavity region of liner 527 were designed with $\sigma = 0.15$ and with thicknesses of 0.040 in. (1.0 mm) each, so as to provide roughly the same flow resistance as the five perforated plates of liner 529. Hence, the possibility that the liner 529 data are significantly in error has been largely dispelled.

One should note that if the perforated plates were removed from the liner cavities so that only air space remained, or, in other words, if $\Omega = s = 1.0$ and $r = 0$, the liner characteristics would be much different than in Figs. 13 and 14. Hence, the perforated plates have some effect on liner performance which is not understood, particularly in view of the fact that the effect is in the direction of reducing the magnitude of J near $kb = 1.0$. With the siren off, the flow noise levels on the surface of liner 529 were 97,220 and 245 Pa for $M_\infty = 0.2$, 0.4, and 0.6, respectively.

A Comparison of Porous and Air-Filled Liners

The amplitude and argument of the impedance of liner 519 is plotted as a function of kb in Figs. 15 and 16. For comparison, the impedance of an air-filled liner, called liner A, is shown in Figs. 17 and 18. Both liners have a surface plate with the same reactance χ_s, but the liner A surface plate has a resistance θ_s, which has been varied as shown on the figures in order to show the effects of changes in θ_s. Since θ_s is a function of both θ_0 and M_∞, a change in θ_s is equivalent to some change in the surface sheet resistance θ_0, and/or a change in M_∞.

At low frequencies, $kb < 0.4$, both liners have $|\zeta|$, which is dominated by the cotkb term in the formula for the reactance of an air column of height b; also, Figs. 16 and 18 show that Arg ζ is approximately the same in this range of kb if θ_s is near 1.7 for liner A. At high frequencies, $kb > 1.2$, liner A is very ineffective as an absorber because Arg ζ is either near 0 or positive, whereas Arg ζ should have a negative value of 15 to 50 degrees for good absorption according to the equations for sound attenuation in a duct.[19] In addition, good sound absorption requires that $|\zeta|$ be near 1.2 $(H/2\pi b)$ (kb), where H is the height of a rectangular duct, implying that H/b should be of the order of 12 at $kb = 1$ for liner 519, and, for the same application, θ_s of liner A should be on the order of 2.

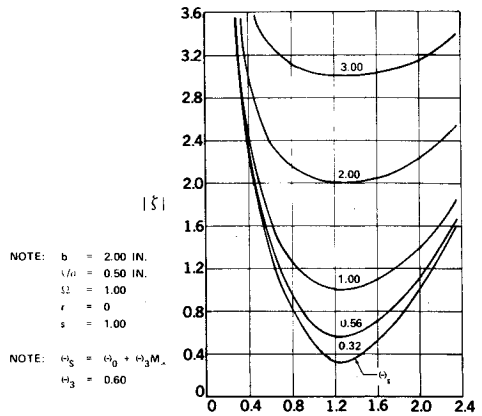

Fig. 17 Calculated $|\zeta|$ vs kb for liner A.

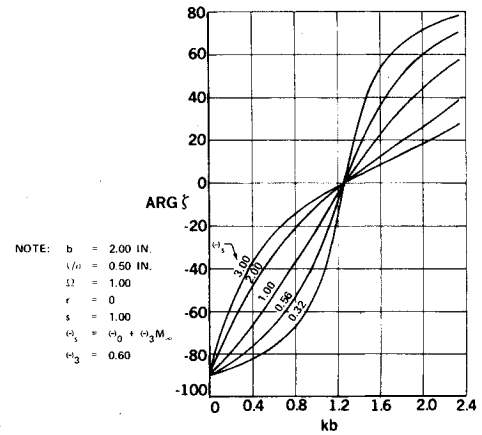

Fig. 18 Calculated Arg ζ vs kb for liner A.

In general, it can be said for H/b near 12 and for an optimum θ_s for liner A that the absorptive performance of both liners will be about equal and will have peak attenuation for kb in the range of 0.4 to 1.2. For $kb<0.4$, both liners are about the same, but their absorptivity is small. For $kb>1.2$, liner 519 has moderate absorptive performance, whereas liner A has very poor performance. Hence, the porous liner has a much wider frequency range for sound absorption than does the air-filled liner.

Conclusions

A mathematical model of porous, point-reacting acoustic liners has been developed and compared with results of testing liner panels using the two-microphone technique. The main conclusions are as follows:

1) The mathematical model shows good agreement with experimental results. The porous liner is much more absorptive at high frequencies than an air-filled liner.

2) Tests of multilayer liners, made up of alternate layers of air and perforated plates, have shown that the liners do not perform in the manner predicted by the porous liner mathematical model. A new model needs to be developed to explain the apparently contradictory nature of the experimental results.

3) Self-generated noise can be a problem for liners with perforated surface sheets. The problem can be alleviated by using sufficiently small holes in the surface sheet, but more work needs to be done to predict self-noise sound pressure levels.

4) Mathematical models of liner surface sheet impedance have been established for perforated sheets having hole diameters of approximately 0.040 in. (1.0 mm) or larger, but more work needs to be done, both theoretically and experimentally, to evaluate the impedance of porous sheets, in particular where the hole sizes are much smaller than 0.040 in.

References

[1] Nayfeh, A. H., Kaiser, J. E., and Telionis, D. P., "Acoustics of Aircraft Engine-Duct Systems," *AIAA Journal*, Vol. 13, Feb. 1975, pp. 130-153.

[2] Dean, P. D., "An *in situ* Method of Wall Acoustic Impedance Measurement in Flow Ducts," *Journal of Sound and Vibration*, Vol. 34, May 1974, pp. 97-130.

[3] Bauer, A. B. and Chapkis, R. L., "Noise Generated by Boundary Layer Interaction With Perforated Acoustic Liners," *Journal of Aircraft*, Vol. 14, Feb. 1977, pp. 157-160.

[4] Willmarth, W. W., "Pressure Fluctuations Beneath Turbulent Boundary Layers," *Annual Review of Fluid Mechanics*, Vol. 7, 1975, pp. 13-38.

[5] Plumblee, H. E., Dean, P. D., Wynne, G. A., and Burrin, R. H., "Sound Propagation in and Radiation from Acoustically Lined Flow Ducts: A Comparison of Experiment and Theory," NASA Rept. CR-2306, Oct. 1973.

[6] Zwikker, C. and Kosten, C. W., *Sound Absorbing Materials*, Elsevier Publishing Co., New York, 1949.

[7] Bauer, A. B., "Measurements of Lining Impedance in a Duct With Flow," presented to the Acoustical Society of America, Douglas Paper 6419, Nov. 1975.

[8] Bell, W. A., Daniel, B. R., and Zinn, B. T., "Acoustic Liner Performance in the Presence of a Mean Flow and Three-Dimensional Wave Motion," AIAA Paper No. 74-61, Jan. 1974.

[9] Rice, E. J., "A Model for the Pressure Excitation Spectrum and Acoustic Impedance of Sound Absorbers in the Presence of Grazing Flow," AIAA Paper No. 73-995, Oct. 1973.

[10] Rice, E. J., Feiler, C. E., and Acker, L. W., "Acoustic and Aerodynamic Performance of a 6-Foot-Diameter Fan for Turbofan Engines," NASA TN D-6178, Feb. 1971.

[11] Rice, E. J., "A Theoretical Study of the Acoustic Impedance of Orifices in the Presence of a Steady Grazing Flow," presented to the Acoustical Society of America, NASA Rept. TM X-71903, April 1976.

[12] Ingard, U., "On the Theory and Design of Acoustic Resonators," *Journal of the Acoustical Society of America*, Vol. 25, Nov. 1953, pp. 1037-1067.

[13] Zinn, B. T., "A Theoretical Study of Non-Linear Damping by Helmholtz Resonators," *Journal of Sound and Vibration*, Vol. 13, Nov. 1970, pp. 347-356.

[14] Feder, E., "Effect of Grazing Flow Velocity on the Steady Flow Resistance of Duct Liners," Pratt and Whitney Aircraft Rept. 5051, July 1974.

[15] Budoff, M. and Zorumski, W. E., "Flow Resistance of Perforated Plates in Tangential Flow," NASA Rept. TM X-2361, Oct. 1971.

[16] Rogers, T. and Hersh, A. S., "The Effect of Grazing Flow on Steady State Resistance of Square-Edged Orifices," AIAA Paper No. 75-493, April 1975; also, see NASA Rept. CR-2681, April 1976.

[17] Dean, L. W., "Coupling of Helmholtz Resonators to Improve Acoustic Liners for Turbofan Engines at Low Frequency," NASA Rept. CR-134912, PWA-5311, May 1976.

[18] Garrison, G. D., "Suppression of Combustion Oscillations with Mechanical Damping Devices, Interim Report," PWA FR-3299, Pratt and Whitney Aircraft, West Palm Beach, Fla., Aug. 1969.

[19] Cremer, L., "Theorie de Luftschall-Dampfung in Rechteckkanal mit Schuluckender Wand und das sich dabei ergebende hochste Dampfungsmass," *Acustica*, Vol. 3, Beiheft 2, 1953, p. 249.